External and internal wetting of carbon nanotubes with organic liquids

Asa H. Barber,[1] Sidney R. Cohen,[2] and H. Daniel Wagner[1]
[1]*Department of Materials and Interfaces, Weizmann Institute of Science, Rehovot 76100, Israel*
[2]*Chemical Research Support, Weizmann Institute of Science, Rehovot 76100, Israel*
(Received 19 June 2004; revised manuscript received 4 October 2004; published 31 March 2005)

Individual multiwalled carbon nanotubes were controllably wetted by polyethylene glycol, glycerol, and water. A Wilhelmy force balance approach was used to calculate contact angles at the nanotube-polyethylene glycol and nanotube-glycerol interfaces, allowing examination of the contact angle dependence on the nanotube diameter. Water, however, exhibited a significantly larger interaction with the nanotube, which could only be explained by allowing for internal wetting of the open carbon nanotube structure. This internal wetting angle is smaller than the external one.

DOI: 10.1103/PhysRevB.71.115443 PACS number(s): 68.08.Bc, 81.05.Tp, 81.07.De

I. INTRODUCTION

Carbon nanotubes have shown potential as a reinforcing phase in polymer composites due to the excellent mechanical properties of the tube's almost perfect, defect-free carbon structure.[1] For effective reinforcement of a polymer during mechanical loading, stress is to be transferred from the matrix to the nanotube through the interface. Interfacial adhesion is required to be strong enough to allow this transfer of stress, and arises from a variety of mechanisms. Wetting of the reinforcement by the liquid polymer has been widely acknowledged to be a requirement for good adhesion.[2] While wetting of microscopic fibers has been investigated for a number of years, carbon nanotubes present further challenges due to their size.

Contact angle measurements of liquid droplets on fiber surfaces can be used to characterize the wetting behavior of the fiber using optical microscopy. However, the resolution required to observe droplets on carbon nanotubes requires electron microscopy techniques. Recent work[3] has shown that liquid water can be successfully imaged within a carbon nanotube using transmission electron microscopy (TEM). Although the study revealed qualitatively that water appears to wet the interior of the carbon nanotube, using a relatively high vapor pressure liquid in the high vacuum conditions of a TEM chamber gives rise to uncertainties in the wetting behavior, since the liquid tends to evaporate. Further experimental work has also been qualitative in nature and comes almost exclusively from observations of polymer contact angles from polymer nanocomposites.[4–6] These studies show a small polymer contact angle on the nanotube surface, indicating that the nanotubes are indeed easily wetted by the polymer matrix. This also corresponds well with nanomechanical tests of individual nanotube-polymer interfaces, where the interfacial strength in a MWCNT-epoxy and MWCNT-polyethylene-butene system was shown to be substantial.[7,8]

Recently, we have shown that liquid contact angles with carbon nanotubes can be successfully measured in air by recording wetting forces in a scanning force microscope (SFM).[9] The application of a Wilhelmy force balance on the partially immersed nanotube can then be used to calculate the liquid equilibrium contact angle on the nanotube surface. This was used to fully characterize the wetting behavior of a closed (capped) multiwalled carbon nanotube (MWCNT). Here, we extend the previous work to examine the wetting properties of open carbon nanotubes of varying diameter, bearing in mind that internal wetting of open nanotubes could provide a mechanism for enhancing the interfacial strength.

II. EXPERIMENT

The MWCNTs used throughout this work were from Sun Nanotech Co. Ltd., China. Purification of the nanotubes was carried out by refluxing the nanotubes in dilute nitric acid for 18 h, followed by oven drying. The resultant purified nanotubes were free of metal catalyst particles with the acid treatment also causing mild oxidation of the nanotube. TEM micrographs in Fig. 1 show the acid treatment results in opening of the ends of the nanotubes. Purified nanotubes were attached to the tip of an atomic force microscope (AFM) cantilever using a previous method.[10] It was found that short or badly aligned nanotubes attached to the AFM tip could not be used for wetting studies because of a tendency for the probe liquid to wet both the nanotube and the silicon tip and cantilever. Therefore, nanotubes with a length exceeding 1 μm and a range of diameters of 20, 40, and 60 nm were selected.

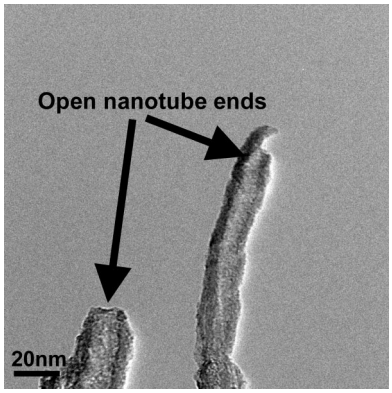

FIG. 1. TEM micrographs of typical CVD powder showing an opening of MWCNTs due to chemical treatments.

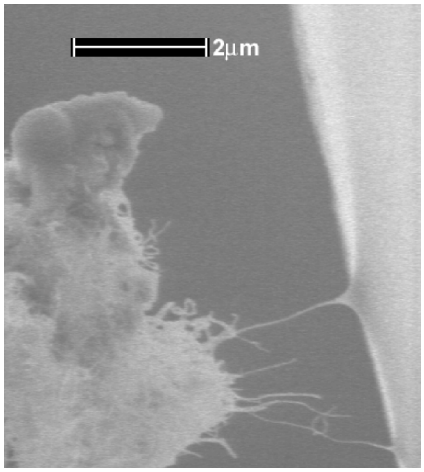

FIG. 2. ESEM micrograph of a MWCNT contacting a liquid surface.

Each nanotube-AFM probe was lowered separately into liquids of polyethylene-glycol, glycerol, and water using an SFM (NT-MDT, Russia). These liquids were used so that the wetting behavior between carbon nanotubes and liquids with a relatively large range of surface tension values (48.3 mJ m^{-2}, 64.0 mJ m^{-2}, and 72.8 mJ m^{-2} for PEG, glycerol, and water, respectively[9]) could be evaluated. Each liquid is also mutually soluble within the other, thus any liquid residues on the nanotube surface would not affect further wetting experiments when using another liquid. Lowering of the nanotube-AFM probe was performed using a noncontact AFM mode until the magnitude of the oscillation signal dropped by approximately 30%, indicating a close proximity of the tip to the liquid surface. The probe modulation was then disabled and the nanotube-AFM probe moved slowly toward the liquid surface using the AFM z-piezo while monitoring the cantilever deflection signal. An abrupt change in the deflection signal indicated that the nanotube had been partially pulled into the liquid due to the wetting forces between the tube and liquid. This was observed for all of the liquids with all of the nanotubes, which is qualitative proof that carbon nanotubes are at least partially wetted by the organic liquids and have hydrophilic characteristics, in contrast to the general hydrophobic behavior of graphite.[11] The deflection signal was converted to force after measuring the spring constant of each cantilever used employing the Sader method.[12]

The liquid-NT contact was independently visualized by contacting bundles of MWCNTs with liquids in an environmental scanning electron microscope (ESEM, XL-30, Philips). An example of this is given in Fig. 2, which shows a single MWCNT from a nanotube bundle contacting a glycol liquid surface. This highlights how the nanotube is wetted by the liquid and no bending of the tube occurs at this liquid surface. Each nanotube-AFM probe was left in a given liquid for 10 s. During this time, the cantilever deflection signal remained constant. This indicates that equilibrium conditions were reached rapidly and no dynamic events, such as a change in the contact angle which would affect the wetting forces acting on the nanotube, occurred within this time interval. Subsequent removal of the nanotube-AFM probe was achieved by retraction of the AFM z-piezo.

III. ANALYSIS

Upon contact with a liquid, the nanotube is pulled into the liquid but restrained from becoming completely immersed due to the restoring force of the bent cantilever. Thus, the bending force was equal but opposite to the attractive forces applied on the nanotube from the wetting and capillary forces of the liquid. This force balance has been previously applied to a number of different geometries, such as fibers or plates, and is typically known as a Wilhelmy plate or balance method. In its basic form, the Wilhelmy balance method relates the restoring force at equilibrium F_r, measured in our experiments from the cantilever bending, to the contact angle of the liquid on a solid cylindrical surface. Therefore, when the surface tension acting on the outer surface of the nanotube, F_{out}, is the only liquid force acting on the tube, then $F_r = F_{out}$ and

$$F_{out} = \gamma_\ell \pi d_{out} \cos \theta_{out}, \tag{1}$$

where γ_ℓ is the liquid surface tension, d_{out} is the outer nanotube diameter, and θ_{out} is the contact angle of the liquid with the nanotube surface. It should also be noted that Eq. (1), which originates from macroscopic wetting behavior, is not obviously valid at the nanolevel. In particular, line tension effects have been suggested to modify the contact angle of small liquid volumes on surfaces.[13] Previous experiments[14] have measured the contact angles of micron-sized and nanosized alkane droplets partially wetting a chemically treated silicon substrate. This work found that surface heterogeneities, and *not* line-tension effects, were responsible for differences in contact angle values. Previous experimental evaluation of contact angles for liquids on 20 nm diam nanotube surfaces[9] successfully used Eq. (1), showing good agreement with theoretical work.[15] Therefore, based on these previous studies, we assume that Eq. (1) will hold for the dimensions of nanotubes used within this work.

When open nanotubes contact a liquid surface, internal wetting of the open tube must be considered. This internal wetting force, F_{in}, due to the liquid surface tension acting on the nanotube interior surface and pulling the nanotube into the liquid also takes the form of Eq. (1), thus

$$F_{in} = \gamma_\ell \pi d_{in} \cos \theta_{in}, \tag{2}$$

where d_{in} is the internal carbon nanotube diameter and θ_{in} is the internal liquid contact angle. The total force acting on the nanotube and pulling it into the liquid will be dominated by internal and external nanotube wetting. The restoring force, F_r, associated with the AFM cantilever bending is equal but opposite to the sum of all of the wetting forces due to the action of the liquid on the nanotube, giving

$$F_r = F_{out} + F_{in}. \tag{3}$$

Substituting Eqs. (1) and (2) into Eq. (3) gives

$$F_r = \gamma_\ell \pi (d_{out} \cos \theta_{out} + d_{in} \cos \theta_{in}). \tag{4}$$

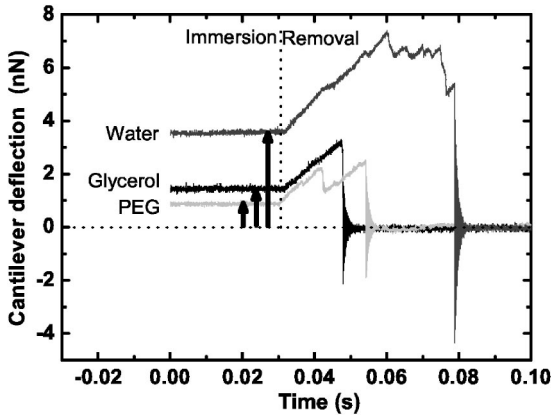

FIG. 3. Immersion and removal of individual CVD grown nanotubes, in this case CVD-20 MWCNTs, from various probe liquids.

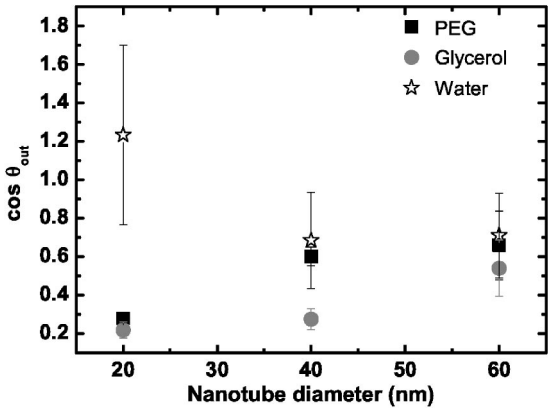

FIG. 5. Plot of cos θ_{out}, calculated from Eq. (1) against the type of nanotube used during wetting experiments.

IV. RESULTS AND DISCUSSION

The partial immersion and removal of individual nanotubes from the three differing probe liquids is monitored by measuring the cantilever deflection signal. Typical forces acting on individual nanotubes during the immersion and removal process are shown in Fig. 3. The far left of each plot shows the force (F_r) acting on the nanotube when the latter is partially immersed in the liquid. This force is constant due to the wetted nanotube being in equilibrium with the liquid, and the magnitude of F_r is indicated by the arrows shown in Fig. 3. Removal of the nanotube results in an increase in the force acting on the nanotube. This force continues to increase until the nanotube is fully removed from the liquid and the force acting on the nanotube then falls to zero. The force F_r depends on the nanotube diameter, as shown in Fig. 4, and generally increases with the diameter, in agreement with Eq. (1).

The contact angles between carbon nanotubes and the probe liquid can be calculated from Eq. (1) using the measured forces shown in Fig. 4. As Eq. (1) considers wetting of the external nanotube surface only, a plot can be made of the external wetting angle for the various liquids used against nanotube diameter (Fig. 5). In addition, the average wetting angles are listed in Table I, and show similar trends to previous work,[9] i.e., increasingly polar liquids give progressively larger contact angles on the nanotube surface. The carbon nanotubes used in this study, grown by CVD methods, are high in defects as highlighted by their irregular wall structure shown in the TEM micrograph in Fig. 1. From Fig. 5 and Table I, the wetting angle with PEG becomes progressively smaller as the nanotube diameter increases. This trend is also exhibited with glycerol as a probe liquid. For the largest nanotube diameters (60 nm), the PEG and glycerol wetting angles are significantly smaller than the contact angles measured for arc-discharge grown nanotubes,[9] which have a more regular structure. This indicates that possible high-energy defect sites are responsible for enhanced wetting for the higher defect density CVD grown nanotubes, compared to arc-discharge grown nanotubes.[9] Indeed, classical work by Wenzel[16] shows how liquid contact angles decrease on roughened surfaces, i.e., more surface defects introduced to the surface. Since the total number of defects at the nanotube surface will also increase as the nanotube diameter in-

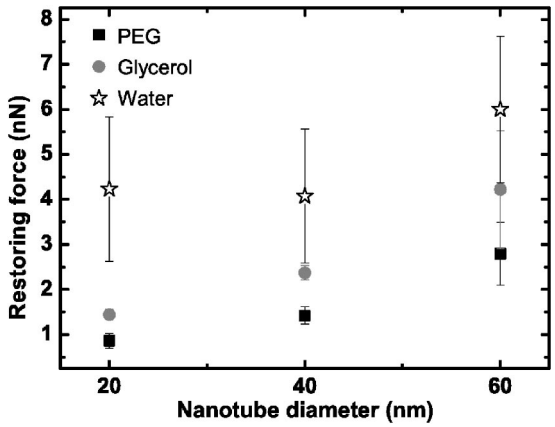

FIG. 4. Plot of force acting on a nanotube during partial immersion (F_r) in various liquids at equilibrium.

TABLE I. Measured contact angles for nanotubes of various diameters partially wetted by differing organic probe liquids. Note that the ranges of wetting angles for water calculated from Eq. (4) using the limit of θ_{out} for water must be larger than θ_{out} for glycerol. Note: an asterisk denotes "assumed." See text.

Probe liquid	Nanotube external diameter (nm)	Contact angle (deg)	
		External, θ_{out}	Internal, θ_{in}
PEG	20	73±2	
	40	53±3	
	60	49±12	
Glycerol	20	77±3	
	40	74±3	
	60	57±10	
Water	20	>77*	0
	40	>74*	0–66
	60	>57*	0–104

creases, the wetting properties of CVD grown nanotubes will be governed by the number of defects at the nanotube surface. Thus, carbon nanotubes with large diameters, containing a high number of surface defects, will give smaller liquid contact angles when compared to thinner nanotubes. This explanation is further supported when comparing contact angles in this work with previous contact angles on arc-discharge grown carbon nanotubes.[9]

Water presents problems when calculating contact angles using the same methods as for PEG and glycerol. The forces acting on the nanotube during partial immersion in water are insufficiently described using Eq. (1). This is evident from the plot in Fig. 5 as the cos θ values for water are either very close to 1, indicating that water spontaneously wets the outer surface of a nanotube with a contact angle of 0 (deg) (in contrast to previous work[9]), or are unphysical for cos $\theta > 1$. A simple way to resolve this issue is to consider that the wetted perimeter must be larger than just the outer perimeter considered in Eq. (1). This can occur if there is significant wetting of the inner nanotube, a phenomenon that has been previously observed for multiwalled nanotubes[3] and more recently for carbon nanopipes[17] using electron microscopy as well as being predicted from simulation work.[18] We therefore assume that the forces acting on the nanotube result from the liquid surface tension at both the external and internal surfaces of the nanotube. Therefore, a plot can be made of θ_{out} against θ_{in} (Fig. 6) using Eq. (4) and the (constant) force (F_r) acting on the nanotube in water, taken from Fig. 4. The ratio of the outer nanotube diameter to inner nanotube diameter is taken to be $2.5(\pm 0.4):1$, based on TEM pictures of the nanotubes (Fig. 1). Equation (4) possesses two unknowns, θ_{out} and θ_{in}, and only the force is a measurable quantity. Since it is known[9] that the contact angle of water on the outer nanotube surface is larger than the glycerol contact angle, a range of internal contact angles can be produced for water at each diameter, as in Table I.

These results show that the forces pulling open carbon nanotubes into a liquid increase drastically for water when compared with PEG or glycerol. The increase in the pull-in force is attributed to internal wetting with the water only, with the resultant calculated contact angles indicating that internal nanotube wetting with water is more favorable than wetting of the external surface. This difference in internal versus external wetting for water and no internal wetting for PEG and glycol indicate that the internal surface properties of the nanotube surface are markedly different from that of the outer surface. While it is beyond the scope of this work, the presence of defects or different surface chemistry inside the nanotube could all contribute to the observed wetting behavior.

Our results also show how the nanotube diameter can dictate wetting behavior of the nanotube. For PEG and glycerol, the external contact angle generally decreases as the nanotube diameter gets larger. This would indicate that, as well as differences in wetting behavior between external and internal surfaces, the surface wetting properties are dependent on the curvature, or diameter, of the nanotube itself. In contrast to external nanotube wetting, internal wetting with water is more favorable as the nanotube diameter decreases, although the internal wetting of relatively large nanotube diameters is more difficult to evaluate from this work due to the large variability [0–104 (deg)] in the calculated θ_{in} values (see Fig. 6).

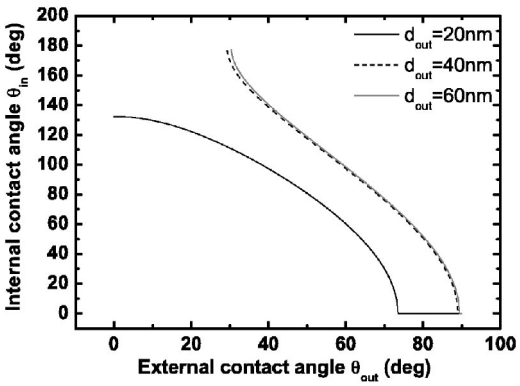

FIG. 6. Variation of internal contact angle θ_{in} with external contact angle θ_{out} using Eq. (4).

V. CONCLUSIONS

Wetting experiments were performed with single carbon nanotubes and various organic liquids. A Wilhelmy force balance method was used to determine the external wetting angles of these nanotubes with PEG and glycol. Since nanotubes with larger diameters have a higher defect density on the external surface, these angles are found to depend on the external nanotube diameter. In water, the wetting forces acting on a nanotube are dominated more by the contribution from internal wetting. These internal contact angles are generally smaller than external contact angles for various nanotube diameters.

ACKNOWLEDGMENTS

This project was supported by the (CNT) Thematic European network on "Carbon Nanotubes for Future Industrial Composites" (EU), the Minerva Foundation and the G. M. J. Schmidt Minerva Centre of Supramolecular Architectures, and the Israel Science Foundation (Grant No. 290/02). We are grateful to S. Safran, P. Pincus, and M. Levy for their stimulating discussions and J. E. Sader for providing software for cantilever calibration.

[1] P. M. Ajayan, L. S. Schadler, and P. V. Braun, *Nanocomposite Science and Technology* (Wiley-VCH, Weinheim, 2003), Chap. 2.
[2] F. Hoecker and J. Karger-Kocsis, J. Appl. Polym. Sci. **59**, 139 (1996).
[3] Y. Gogotsai, J. A. Liberia, and M. Yoshimura, J. Mater. Res. **15**, 2591 (2000).
[4] W. Ding *et al.*, Nano Lett. **3**, 1593 (2003).
[5] E. Assouline *et al.*, J. Polym. Sci., Part B: Polym. Phys. **41**, 520 (2003).
[6] O. Lourie and H. D. Wagner, Appl. Phys. Lett. **73**, 3527 (1998).
[7] C. A. Cooper, S. R. Cohen, A. H. Barber, and H. D. Wagner, Appl. Phys. Lett. **81**, 3873 (2002).
[8] A. H. Barber, S. R. Cohen, and H. D. Wagner, Appl. Phys. Lett. **82**, 4140 (2003).
[9] A. H. Barber, S. R. Cohen, and H. D. Wagner, Phys. Rev. Lett. **92**, 186103 (2004).
[10] H. Nishijima *et al.*, Appl. Phys. Lett. **74**, 4061 (1999).
[11] A. W. Adamson, *Physical Chemistry of Surfaces*, 5th ed. (Wiley, New York, 1990), p. 397.
[12] J. E. Sader, J. W. M. Chon, and P. Mulvaney, Rev. Sci. Instrum. **70**, 3967 (1999).
[13] A. Amirfazli and A. W. Neumann, Adv. Colloid Interface Sci. **110**, 121 (2004).
[14] A. Checco and P. Guenoun, Phys. Rev. Lett. **91**, 186101 (2003).
[15] A. V. Neimark, J. Adhes. Sci. Technol. **13**, 1137 (1999).
[16] R. N. Wenzel, Ind. Eng. Chem. **28**, 988 (1936).
[17] M. Pia Rossi *et al.*, Nano Lett. **4**, 989 (2004).
[18] S. Supple and N. Quirke, J. Chem. Phys. **121**, 8571 (2004).